Studies of a polymeric chromium phosphinate: Structure and static magnetic properties

R. E. Stahlbush, C. M. Bastuscheck, A. K. Raychaudhuri, and J. C. Scott
Materials Science Center and Department of Physics, Cornell University, Ithaca, New York 14853

D. Grubb
Materials Science Center and Department of Materials Science and Engineering, Cornell University, Ithaca, New York 14853

H. D. Gillman
Pennwalt Technological Center, King of Prussia, Pennsylvania 19406
(Received 13 August 1980)

The semicrystalline polymer, poly(chromium bismethylphenyldioctyl-phosphinate), PCrP-C, contains $S=\frac{3}{2}$ chromium ions coupled by Heisenberg antiferromagnetic exchange ($J/k=-2.5$ K) along the linear molecule. We present susceptibility and specific-heat data on pressed sheet samples. X-ray diffraction shows that there is preferential alignment of the molecules in the plane of the sheets, and allows an analysis of the resulting magnetic anisotropy. There is an easy plane perpendicular to the molecular axis and the anisotropy parameter ($D/k\simeq-0.03$ K) is such that a crossover from Heisenberg to XY behavior is observed as the temperature is lowered. There is no evidence for three-dimensional ordering above 20 mK. The effect of an applied magnetic field is to induce a flopped spin alignment in the one-dimensional short-range-ordered regime. We present a calculation, based on a transfer-matrix technique to include both magnetic field and anisotropy within a classical Heisenberg model, giving good semiquantitative agreement with the experimental data.

I. INTRODUCTION

One-dimensional magnetic systems have been, in recent years, a fruitful area of study, providing experimental tests of soluble model Hamiltonians and revealing several phenomena arising directly from the reduced dimensionality.[1-4] Initially the major effort was devoted to identifying materials which exemplified the various symmetries of spin interaction (Heisenberg, XY, Ising) different spin values ($S=\frac{1}{2},1,\ldots$) and the two signs of exchange (ferromagnetic and antiferromagnetic).[1] In most materials studied to date the anisotropy has been sufficiently large or sufficiently small that a clear distinction between the spin dimensionalities can be made. In this paper we explore the phenomena associated with intermediate anisotropy.

First, let us establish what is meant by "sufficiently large," "intermediate," and "sufficiently small" anisotropy. The interaction of the magnetic ion with the electric fields of the ligands around it and an applied magnetic field (H) is parametrized in the single-site spin Hamiltonian

$$\mathcal{H}_{\text{ion}}=-\mu_B\vec{S}\cdot\tilde{g}\cdot\vec{H}-DS_z^2+E(S_x^2-S_y^2)+\cdots, \quad (1.1)$$

where S is the (effective) spin value, $\tilde{g}$ is a tensor, and D and E are the anisotropy parameters.[5] In one-dimensional magnetic systems each ion moment interacts with its neighbors along the chain via exchange,[6] J

$$\mathcal{H}_e=-2J\sum_i\vec{S}_i\cdot\vec{S}_{i+1}\ . \quad (1.2)$$

If D is positive ("easy-axis" anisotropy) and much larger in magnitude than J it is customary to neglect matrix elements in $\mathcal{H}_e$ involving the x and y components of the spins and to write the effective Ising Hamiltonian[7]

$$\mathcal{H}_e'=-2J\sum_i S_i'^zS_{i+1}'^z\ . \quad (1.3)$$

Conversely for negative D ("easy plane") much larger than $|J|$, and for E small, the XY model[8] is appropriate. So we conclude that sufficiently large means $|D|\gg|J|$. In addition $|D|$ should be large compared to the temperatures at which experiments are performed.

A particularly important phenomenon in one-dimensional magnets is the absence of long-range order above absolute zero.[9,10] However, in a real material the interchain interactions can never be completely ignored. If this coupling is characterized by an exchange interaction J' then mean-field

theory[11,12] shows that for Heisenberg intrachain exchange a phase transition to a three-dimensional (3D) long-range-ordered state occurs at a temperature $T_{3D} \sim (|JJ'|)^{1/2}/k$. One-dimensional short-range order starts to build up below the mean-field temperature $T_{MF} \sim |J|/k$, hence there is a regime of one-dimensional critical fluctuations in the temperature range $T_{3D} \lesssim T \lesssim T_{MF}$. It has become customary[1] to gauge the degree of one dimensionality in terms of the ratio T_{MF}/T_{3D} which approaches 10^2 for the "best" examples.

We now argue that sufficiently small anisotropy requires that D and/or E be less in magnitude than J'. Consider specifically an antiferromagnetic chain, $J < 0$, with easy-axis anisotropy, $D > 0$. It is well known that below the three-dimensional Néel temperature there will be a spin-flop transition[13] for a magnetic field applied parallel to the easy axis: $H_{SF} \sim \sqrt{|JD|}/\mu_B$. As we shall show in detail below, in the regime of one-dimensional short-range order there may be sufficient correlation along the chain that a similar phenomenon occurs (through the transition is, of course, not sharp in the one-dimensional case, and the high- and low-field regions are not distinct phases in the thermodynamic sense). If the sum of anisotropy energies (i.e., D times the number of spins) within a coherence length, ξ, is comparable to the thermal energy then the spins within that length will tend to align with the easy axis. If $|D| < |J|$ then at temperatures $T \lesssim T_{MF}$ the Heisenberg expression for the correlation length is appropriate: $\xi \sim (|J|/kT)a$ (a is the lattice spacing) and the total anisotropy energy within a correlation length is $|D|\xi/a \sim |DJ|/kT$. Hence the anisotropy becomes important in comparison with the thermal energy below a temperature T_A such that $|DJ|/kT_A \sim kT_A$; i.e., $T_A \sim \sqrt{|JD|}/k$. Around this temperature there is a crossover from Heisenberg to Ising behavior, the correlation length grows exponentially with further decreasing temperature, the susceptibility becomes highly anisotropic and spin-flop alignment will be observed for fields $H \gtrsim H_{SF} \sim \sqrt{|JD|}/\mu_B$ applied parallel to the easy axis. This field strength is the same as in the conventional spin-flop transition of three-dimensional antiferromagnets because the argument concerning competition between anisotropy energy and Zeeman energy of the perpendicular spin alignment is still relevant. We emphasize again that there is no longer expected to be a sharp transition from one state to another, but rather a gradual change, smeared by thermal fluctuations.

This qualitative discussion allows us to conclude that the intermediate range of anisotropy is defined by $|J'| \lesssim |D| \lesssim |J|$ in the case of antiferromagnetic chains.

The situation for easy-axis ferromagnetic chains is similar. The temperature below which anisotropy effects appear is again $T_A \sim \sqrt{|JD|}/k$, however the relevant field value is now the anisotropy field $H_A \sim |D|/\mu_B$. In the remainder of this paper we shall concern ourselves exclusively with antiferromagnets.

The situation in the case of easy-plane anisotropy with Heisenberg antiferromagnetic exchange is similar to the easy-axis case. A crossover from isotropic behavior at high temperature to XY-like symmetry will occur around $T_A \sim \sqrt{|JD|}/k$. However, the magnetic field dependence is somewhat altered for continuous symmetry: the magnetic energy now competes with the thermal energy which tends to randomize the spin orientation in the XY plane, rather than with the anisotropy energy of a correlated cluster. Hence the approach to a spin-flopped-type of spin arrangement is characterized by a crossover such that the Zeeman energy of a flopped cluster is comparable to kT. The magnetization of the cluster arises because the spins are canted at an angle $\mu H/J$ away from antiparallelism. Hence, for the J/kT spins in the cluster the Zeeman energy is $H(\mu H/J) \times \mu(J/kT) = (\mu H)^2/kT$, and so $\mu H_{SF} \sim kT$.

These qualitative descriptions are summarized graphically in Fig. 1 for both easy-axis and easy-plane

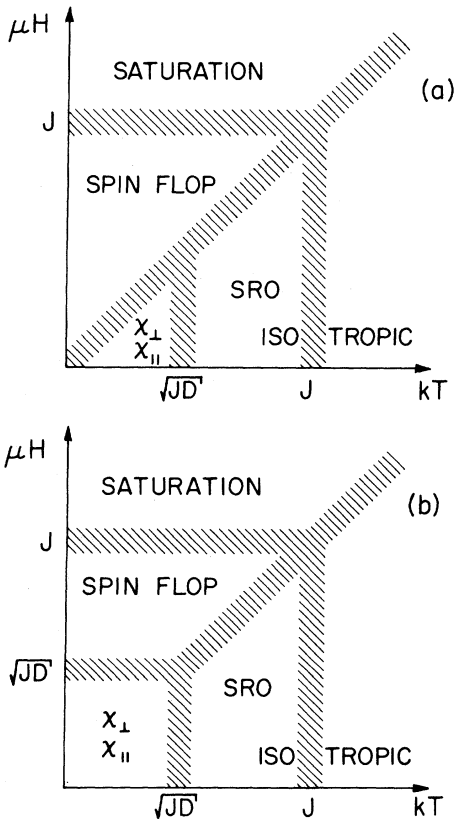

FIG. 1. Schematic representations of the HT plane for one-dimensional antiferromagnets with (a) easy-plane and (b) easy-axis anisotropy. (SRO ≡ short-range order.) The material described in this paper, PCrP-C, corresponds to the case (a).

one-dimensional antiferromagnets.

Many examples of highly one-dimensional magnetic systems have been discussed in the last decade.[1–4] Among the most thoroughly studied are: $(CH)_4NMnCl_3$, (TMMC),[14–22] which is an $S=\frac{5}{2}$ (large enough to be considered a classical rather than quantum spin system) Heisenberg antiferromagnet which shows crossover to XY behavior induced by dipolar interactions[14]; $CsCoCl_3$,[23–27] an $S=\frac{1}{2}$ Ising system; α-CuNSal,[28–33] exemplifying an $S=\frac{1}{2}$ Heisenberg antiferromagnet, and $CsNiF_3$,[34–38] an XY ferromagnet. The ions in these one-dimensional magnets are Mn^{2+} whose spherical symmetry immunizes it from anisotropy effects, Co^{2+} which has unquenched angular momentum in octahedral coordination and is therefore a prime candidate for Ising interactions, Ni^{2+} which has large spin-orbit interactions, and Cu^{2+} which, with its quenched angular momentum $S=\frac{1}{2}$ ground state, exhibits Heisenberg interactions. Intermediate values of anisotropy, $|D|>|J'|$, are more likely to be found in ions with the following properties: nonzero orbital angular momentum quenched by the crystal field of its environment; an excited state, not too high above the ground state, which possesses orbital angular momentum in a cubic environment; coordination which is close to, but not exactly, cubic in order that spin-orbit interactions can produce anisotropy in second order. Both octahedral Cr^{3+} (d^3) and tetrahedral Co^{2+} (d^7) meet these requirements[39] since both have a ${}^4A_{2(g)}$ ground state with an orbital triplet, ${}^4T_{2(g)}$ lying approximately 2 eV higher. The two anisotropy parameters (D and E) are given in second-order perturbation theory by the expressions

$$|D|,|E|\sim\lambda^2\delta_i/\Delta^2 \ , \tag{1.4}$$

where λ ($\sim 10^2$ K) is the spin-orbit coupling, Δ ($\sim 10^4$ K) is the A-T ligand field splitting in a cubic field, and δ_i (typically $\sim 10^3$ K) are the splittings of the excited orbital triplet due to departures from cubic symmetry. Hence $|D|\sim|E|\sim 10^{-1}$ K might be expected. This energy is comparable to the intrachain dipolar coupling which tends to favor XY behavior. The one-dimensional material which contains these ions should therefore have interchain interactions, J', on the order of or less than 10^{-2} K.

In this paper we describe a polymeric phosphinate of chromium (PCrP-C: see Sec. III) which meets all the criteria discussed in the preceding paragraph, and which indeed reveals symmetry crossover behavior in the short-range-ordered paramagnetic phase. We shall show that this is a material with $D<0$ and $E\sim 0$ (effectively) so that the low-temperature behavior is XY-like, and a spin-flopped alignment is achieved for fields $H>>kT/\mu_B$.

Section II contains a more detailed theoretical analysis of these ideas based on a transfer-matrix treatment of the classical Heisenberg chain including both anisotropy and an applied field. In Sec. III we present details of the molecular and magnetic structure of the material studied. Section IV contains a description of the experiments used to reveal the magnetic thermodynamic behavior. The experimental results are presented and discussed in Sec. V, making comparison with the theoretical predictions. Section VI contains a summary.

II. THEORY

The Heisenberg Hamiltonian for a one-dimensional array of spins, $[S_i]$, $i=1,\ldots,N, S_{N+1}=S_1$, including terms for single-site anisotropy (easy axis or easy plane) and the Zeeman interaction, is given by

$$H=-2J\sum_{i=1}^{N}\vec{S}_i\cdot\vec{S}_{i+1}-D\sum_{i=1}^{N}(S_i^z)^2-g\mu_B\vec{H}\cdot\sum_{i=1}^{N}\vec{S}_i \ , \tag{2.1}$$

where J is the exchange energy, D is the single-site anisotropy, and H is the applied field. The Hamiltonian for anisotropic exchange or for dipolar coupling may be rewritten in this form if the anisotropy is small, $|D/J|<<1$.[3,4] The 1D Heisenberg Hamiltonian in zero field has been considered in various analytic approximations[40] and using numerical methods.[41–44] Several exact solutions for the ground-state properties of the quantum chain exist,[45–46] but the only exact results[47–50] for thermodynamic quantities are classical, i.e., all spin commutators are set to zero, which corresponds to having infinite spin. An analytic solution for zero field and no anisotropy was first given by Nakamura[47] and later independently by Fisher.[48] Numerical calculations using the transfer integral technique exist which include either anisotropy or magnetic field. Joyce[49] uses an anisotropic exchange, Loveluck *et al.*[51] include single-site anisotropy, and Blume *et al.*[52] have an applied field. Walker *et al.*[17] apply the results of a transfer-matrix calculation with anisotropic exchange to the susceptibility of TMMC. They discuss, but do not explicitly show, the behavior in a weak magnetic field.

Another classical technique, employed by Selke and Pesch,[53] is the $1/n$ expansion (where n is the spin dimensionality). Perturbation from the spherical model, $n=\infty$, are analytically calculated with an expansion to $1/n$. Their calculation includes both single-site anisotropy and a magnetic field. However, this method should be viewed with suspicion since in the limits of zero field or zero anisotropy, the results only agree qualitatively with the more accurate transfer integral calculations.

As shown by Weng,[54] and later by Blöte,[44,55] the classical susceptibility becomes a better approximation

as the spin of the quantum system increases. We note, in their work, that classical susceptibility never overestimates the spin-$\frac{3}{2}$ result by more than 15%. On the other hand, the classical magnetic specific heat[48] is much less and its application to real systems should be approached with extreme caution.

Encouraged by the accuracy of the classically calculated susceptibility and motivated by the PCrP-C data below, which exhibit anisotropy as well as magnetic field dependence, we undertook a calculation using the transfer integral method in which both terms were included. For classical calculations the Hamiltonian [Eq. (2.1)] is rewritten

$$\mathcal{H}=-2JS(S+1)\sum_{1}\vec{s}_i\cdot\vec{s}_{i+1}-DS^2\sum_{1}(s_i^z)^2 - g\mu_B\sqrt{S(S+1)}H\sum_i s_i^z \ , \tag{2.2}$$

where $\{\vec{s}_i\}$ are unit vectors with commuting components. Setting the magnitude of the spin equal $\sqrt{S(S+1)}$ in the first and third term is a quantum correction. With this "renormalization" and no anisotropy, the high-temperature, $T \gg J$, classical derived susceptibility is the same as its quantum counterpart.

For clarity and completeness, we include a description of the transfer-matrix approach[17] as it applied to the Hamiltonian (2.2). The symmetrized kernel[52]

$$A(\vec{s}_i,\vec{s}_{i+1})=\exp\left[J'\vec{s}_i\cdot\vec{s}_{i+1}+\frac{D'}{2}(s_i^z)^2+\frac{D'}{2}(s_{i+1}^z)^2+\frac{H'}{2}(s_i^z+s_{i+1}^z)\right] \ , \tag{2.3a}$$

$$J'=2JS(S+1)/kT \ , \tag{2.3b}$$

$$D'=DS^2/kT \ , \tag{2.3c}$$

$$H'=g\mu_B[S(S+1)]^{1/2}H/kT \ , \tag{2.3d}$$

enters the partition function

$$Z_N=\int\frac{d\Omega_1}{4\pi}\int\frac{d\Omega_2}{4\pi}\int\cdots\int\frac{d\Omega_N}{4\pi}A(\vec{s}_1,\vec{s}_2)A(\vec{s}_2,s_3)\cdots A(\vec{s}_N,\vec{s}_1) \ , \tag{2.4}$$

which shows that Z_N is formally the trace of the Nth power of A. The eigenvalues λ_n of the integral equation,

$$\int A(\vec{s}_i,\vec{s}_{i+1})\psi_n(\vec{s}_i)\frac{d\Omega_i}{4\pi}=\lambda_n\psi_n(\vec{s}_{i+1}) \tag{2.5}$$

give the partition function in the thermodynamic limit[52]

$$Z=\lim_{N\to\infty}\sum_n(\lambda_n)^N=\lim_{N\to\infty}\lambda_{\max}^N \ . \tag{2.6}$$

Instead of Eq. (2.5), an integral equation with an unsymmetrized kernel was solved, giving an identical eigenvalue spectrum.

The molar magnetic susceptibility and specific heat are given by

$$\chi=N_A kT\frac{d}{dH}\left(\frac{1}{\lambda_{\max}}\frac{d\lambda_{\max}}{dH}\right) \ , \tag{2.7}$$

$$C=N_A k\frac{d}{dT}\left(\frac{T^2}{\lambda_{\max}}\frac{d\lambda_{\max}}{dT}\right) \ , \tag{2.8}$$

where $\lambda_{\max}$ is the largest eigenvalue of (2.5) and N_A is Avogadro's number. The solution in the special case $D'=H'=0$ reproduces Fisher's results.[48] We reproduce it here because the eigenvalue spectrum will be used later. The integral equation reduces to

$$\int\exp(J'\vec{s}_i\cdot\vec{s}_{i+1})Y_{lm}(\Omega_i)\frac{d\Omega_i}{4\pi}=\lambda_{lm}Y_{lm}(\Omega_{i+1}) \ . \tag{2.9}$$

The eigenfunctions are the spherical harmonics Y_{lm} and the eigenvalues are

$$\lambda_{lm}=(\pi/2J')^{1/2}I_{l+1/2}(J') \ , \tag{2.10}$$

where $I_{l+1/2}$ is a modified Bessel function of the first kind:

$$\lambda_{\max}=\lambda_{00}=\frac{\sinh J'}{J'} \ . \tag{2.11}$$

To solve the full kernel, first use the completeness of the spherical harmonics:

$$\psi_n=\sum_{l=0}^{\infty}\sum_{m=-l}^{l}\left[\frac{4\pi}{(2l+1)}\right]^{1/2}B_{lm}^n Y_{lm} \ , \tag{2.12}$$

$$\exp(D'\cos^2\theta+H'\cos\theta)=\sum_{l=0}\left[\frac{4\pi}{(2l+1)}\right]^{1/2}F_l Y_{l0} \ . \tag{2.13}$$

In Eq. (2.13) only the $m=0$ terms need be considered since there is no ϕ dependence. Now, suppose that only one value of m appeared in Eq. (2.13):

$$\psi_{nm}=\sum_{l=0}B_{lm}^n Y_{lm} \ . \tag{2.14}$$

Using the additional theorem, the product of (2.13) and (2.14) can be expressed as an expansion in spherical harmonics.

$$\exp(D'\cos^2\theta+H'\cos\theta)\psi_{nm}=\sum_{l=0}C_{lm}^n Y_{lm} \ . \tag{2.15}$$

Again, only one value of m enters; the integral equa-

tion can now be viewed as having the $D'=H'=0$ kernel, (2.9), operating on (2.15). Since the spherical harmonics are eigenfunctions of the $D'=H'=0$ kernel, spherical harmonics with different m's are not coupled by the full kernel.

Another important simplification occurs since, in one-dimensional systems with short-range interactions, there can be no long-range order at finite temperature. As parameters of the system change (temperature, magnetic field, etc.), a phase transition occurs when the maximum eigenvalue crosses another eigenvalue which then becomes the new largest eigenvalue. When $D'=H'=0$, the largest eigenvalue corresponds to the eigenfunction λ_{00}. As D' and H' are "turned on" the eigenfunction expansion, (2.15) continues to contain only $m=0$. Furthermore, the corresponding eigenvalue remains the largest eigenvalue for all values of D' and H'.

The calculations proceed by operation on Eq. (2.15) (setting $m=0$) with the $D'=H'=0$ kernel. Then, using the orthogonality of the spherical harmonics, the following matrix equation for the eigenvalues, λ_n, is obtained:

$$\sum_{l'=0} M_{ll'} B^n_{l'0} = \lambda_n B^n_{l0} \ , \tag{2.16a}$$

$$M_{ll'} = \lambda_{l0} \sum_{j=|l-l'|}^{l+l'} F_j \langle l|l';j\rangle \ , \tag{2.16b}$$

$$P_l P_j = \sum_{l=0}^{l+j} \langle l|l';j\rangle P_l \ , \tag{2.16c}$$

where λ_{l0}, B^n_0, and F_j are defined in (2.9), (2.12), and (2.13), respectively, and the P's are Legendre polynomials. Since the matrix elements, $M_{ll'}$, decrease as l and l' increase, it is possible, in practice, to truncate the infinite matrix and still obtain an excellent approximation for the largest eigenvalue. To calculate the susceptibility, the maximum eigenvalue is calculated for a sequence of fields and the derivatives in Eq. (2.7) are determined numerically. Similarly, a sequence of temperature points can be used to calculate the specific heat, Eq. (2.8).

As the ratios J/kT and H/kT increase, it is necessary to use larger matrices. With the parameters appropriate to PCrP-C, $J/k=2.78$ K, $D/k=-0.03$ K, and $S=\frac{3}{2}$, a 20×20 matrix gave 1% or better accuracy for the susceptibility (comparing the 20×20 to a much larger matrix) in the temperature and field ranges $T\geq 1$ K and $H\geq 50$ kG. The accuracy in the limit $D=H=0$ was also checked against Fisher's analytic solution[48] and was within 1%. Using a Prime 400 minicomputer, the time to diagonalize the required number of matrices larger than 30×30 starts becoming excessive and is the major limitation imposed on the ratios J/kT and H/kT.

The results of the calculations are displayed in Figs. 2–4. The parameters were chosen in order to facilitate comparison with the corresponding experimental data. Since the magnetic field is always along the z axis the easy-axis case corresponds to a parallel susceptibility and the easy-plane to a perpendicular susceptibility. Thus, we have only theoretical behavior (Fig. 2) for two of the four measurable responses: $\chi_\parallel$ and $\chi_\perp$ for each sign of D. We expect $\chi_\perp(D>0)$ to behave quite similarly to the easy-plane perpendicular susceptibility since both involve competition between Zeeman and anisotropy energy. On the other hand, since the XY system has continuous symmetry, $\chi_\parallel(D<0)$ will be more comparable to the isotropic (Heisenberg) case.

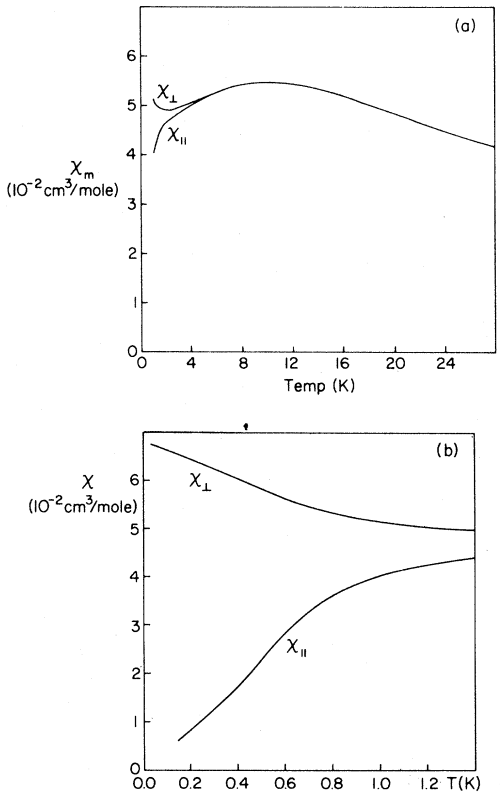

FIG. 2. Temperature dependence of the initial susceptibility for fields applied parallel to the easy axis ($\chi_\parallel$) and perpendicular to the easy plane ($\chi_\perp$) of a one-dimensional classical antiferromagnet: $J/k=-2.8$ K and $|D/J|=10^{-2}$. These values were chosen to facilitate comparison with the experimental data on PCrP-C. (a) and (b) show different temperature scales.

The effect of applied magnetic field is shown in Fig. 3. The increasing susceptibility signals the onset of a flopped spin alignment. At low temperature when $D>0$ a peak begins to develop at $\mu H\cong\sqrt{|JD|}$. This is associated with the increasingly sharp transition to the spin-flopped state of an easy-axis antiferromagnet. By contrast the easy-plane case [Fig. 3(b)] shows no peak because the realignment

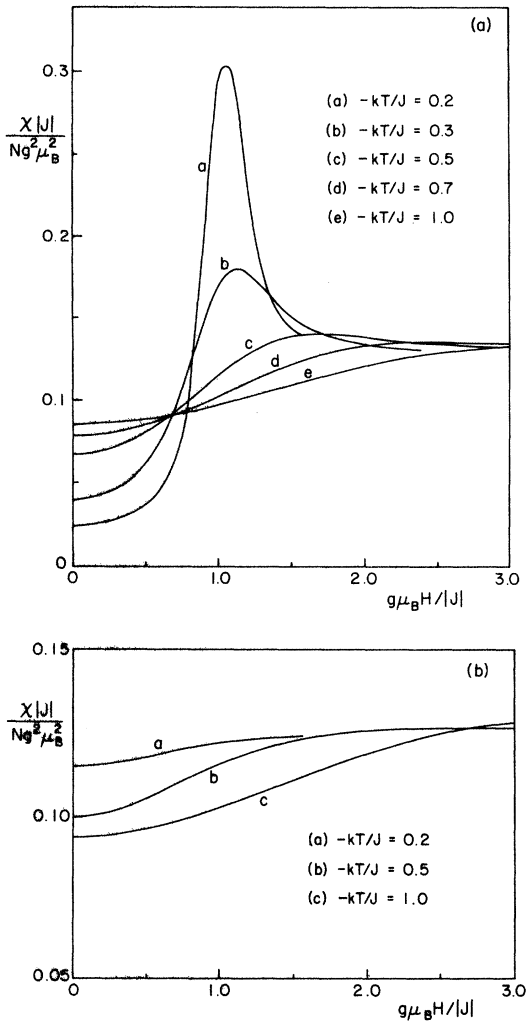

FIG. 3. (a) Field dependence of the susceptibility for easy-axis anisotropy, $D > 0$. $|D/J| = 3 \times 10^{-2}$. (b) Field dependence of the susceptibility for easy-plane anisotropy, $D < 0$. $|D/J| = 2 \times 10^{-2}$.

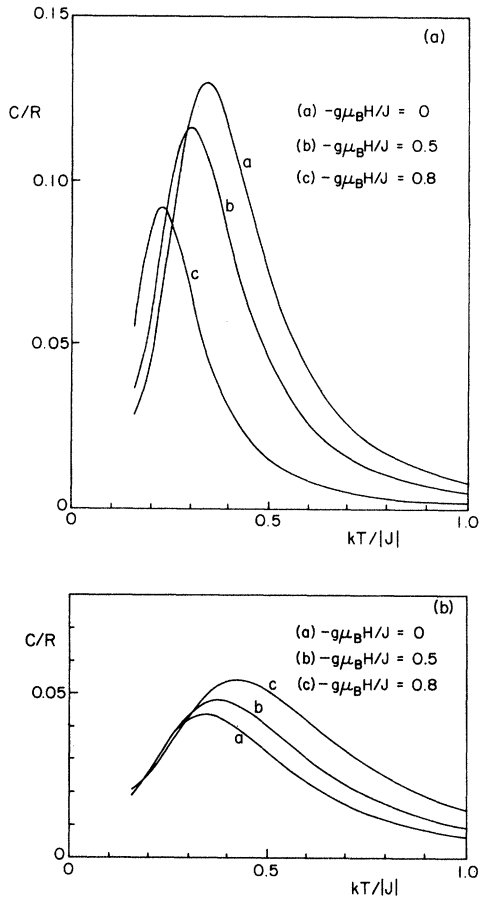

FIG. 4 Excess specific heat (see text) for (a) easy-axis and (b) easy-plane anisotropy at several different fields. $|D/J| = 2 \times 10^{-2}$

takes place continuously with increasing field at all temperatures.

Figure 4 displays the results for the specific heat. We plot the difference in the values with and without anisotropy since we expect that, although the absolute value for the classical calculation is grossly in error at low temperature, the excess specific heat associated with the symmetry crossover should be at least qualitatively correct. Note that for the easy-axis case H, which is parallel to that axis, tends to lower the crossover temperature (i.e., to favor perpendicular spin alignment), whereas for the easy plane the transition to XY behavior is enhanced. This is precisely what one expects on the basis of simple arguments concerning the effect of the Zeeman contribution to the energy balance. Strictly speaking, therefore, the hatched lines at $kT = \sqrt{JD}$ on Fig. 1 should not be vertical.

Note also the difference in magnitude of the excess specific heat for the two cases: it is considerably larger for the easy-axis system. Although we have not examined the entropy change in detail, this behavior is qualitatively what one expects on the basis of the change in number of degrees of freedom for spin orientation.

III. CHARACTERIZATION OF POLY(CHROMIUM PHOSPHINATE)

A. Chemistry

The phosphinate anion, $(OPRR'O)^-$ where R and R' are hydrocarbon groups, is well known to form bridges between transition-metal cations,[56] leading in many cases to a linear polymeric structure in which the magnetic ion is an integral part of the backbone

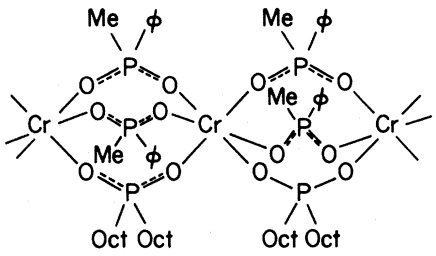

FIG. 5. Molecular structure of poly(chromium-bismethylphenyldioctyl-phosphinate), PCrP-C. *Me* $\equiv CH_3$; $\phi \equiv C_6H_5$; *Oct* $\equiv C_8H_{17}$.

of the molecular chain. Earlier studies[57–60] have shown that the chromium trisphosphinate,[61] $Cr[O_2P(CH_3)(C_6H_5)]_2[O_2P(C_8H_{17})_2]$ is a semicrystalline linear polymer of high molecular weight. [Following Ref. 58 we shall refer to this material as PCrP-C (see Fig. 5).] Samples were prepared in the manner described previously.[61] At the last stage of phosphinate addition, the reaction mixture was pressed to yield flexible sheets of order 0.5 mm thickness, from which specimens were cut.

These sheets were found to form gels readily, absorbing nonpolar solvents such as chloroform and toluene. The expansion associated with this gelation occurs primarily perpendicular to the sheet, indicating a high degree of anisotropy in molecular model structure is highly linear with relatively few cross-links between the individual chains.

B. Structure

X-ray powder-pattern photographs, using Cu K_α (1.54-Å) radiation, were taken with two orientations of the incident beam relative to the sheet. When the incident beam is perpendicular to the sheet [Fig. 6(a)] the scattering is azimuthally symmetric, with sharp diffraction rings corresponding to spacings 4.52(2), 7.81(2), 13.4(1), and 26.8(5) Å. The widths of the 4.52-Å rings correspond to coherence lengths on the order of 100 Å or greater, and may be resolution limited. The other rings are relatively broader. Stretching of the sheet [Fig. 6(b)] produces anisotropy with the intensity of the 4.52-Å scattering concentrating along the axis of alignment, while the remaining features become stronger in the equatorial plane. This behavior indicates that the shortest spacing is in a direction along the molecular chain, while the other values are interchain separations. Comparison of the spacings with the Cr-Cr separation in a crystalline dimeric chromium phosphinate and examination of a molecular model constructed on the basis of phosphinate group geometry known from other crystalline complexes reveals that the 4.52-Å distance should be identified with the distance between chromium atoms along the polymer chain.

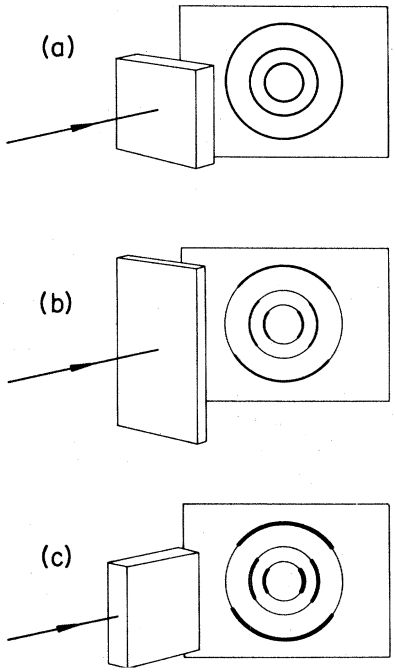

FIG. 6. X-ray diffraction geometry. (a) Normal incidence, unstretched sheet. (b) Normal incidence, sheet aligned by stretching. (c) Parallel incidence.

Diffraction patterns taken with the incident beam parallel to the unstretched sheet [Fig. 6(c)] show considerable anisotropy. The 4.52- Å scattering is concentrated in the plane of the sheet, whereas the 7.81- and 13.4-Å rings are more intense in the perpendicular direction. These features indicate that in the process of pressing the film from the reaction mixture considerable alignment of the molecules takes place, and that the structural coherence is greater along the chain than transversely.

The intrachain Cr-Cr distance, $a = 4.52$ Å, results in a dipole-dipole interaction $g^2\mu_B^2/a^3k = 0.03$ K.

We have made several attempts to align the polymer further by stretching the sheets. As mentioned above, this produces a small amount of anisotropy in the structure, but we have not been able to achieve elongation beyond 180% and the resulting alignments are insufficient to enable detailed analysis of the anisotropy of various physical quantities. On the other hand, the anisotropy produced in pressing the sheets is evident in susceptibility and ESR measurements.

C. Magnetic properties

Low-field static magnetic susceptibility measurements were repeated previously.[58,60] In Fig. 7 we show new data taken in one case with higher resolution than before (using a Faraday balance)[62] and in the other cases to lower temperature (using an ac in-

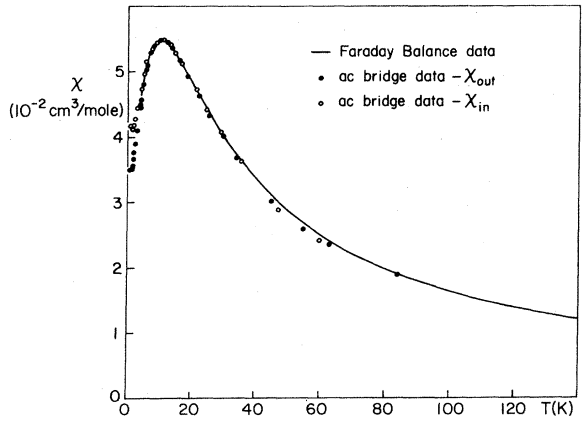

FIG. 7. Initial susceptibility of PCrP-C. The Faraday balance measurements were made on unaligned samples. χ_{out} and χ_{in} refer to ac magnetic field directions out of and in the plane of the sample sheets. For clarity only about half of the ac data points are shown below 20 K.

duction bridge, to be described below). These data reveal the behavior expected of a one-dimensional Heisenberg antiferromagnet. The susceptibility data are discussed in detail below.

ESR spectroscopy, at X band, has been performed.[63] The temperature dependence and the anisotropy of the linewidth will be the subjects of a future publication. In this paper we shall make reference to the g factor: $g=1.974(3)$ and is, within the resolution, isotropic.

D. Optical adsorption

The visible adsorption spectrum of PCrP-C (Fig. 8) shows to two broad bands centered at 15 000 and 22 000 cm^{-1}, which are typical of octahedrally coordinated Cr III, and are responsible for the green color

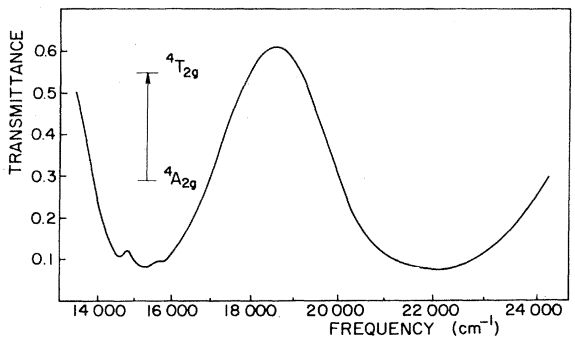

FIG. 8. Optical spectrum of PCrP-C associated with the 15 000-cm^{-1} band.

of the polymer. The 15 000-cm^{-1} band corresponds to the $^4A_{2g}$-$^4T_{2g}$ transition of the chromium ligand field levels.[39] The molecular structure suggests that the threefold orbital degeneracy of the excited $^4T_{2g}$ level is completely removed, the octahedral symmetry of the oxygen ions being distorted along two axes. The chain is one of these axes, as can be demonstrated by building models with the normal phosphinate anion bond lengths and angles. The second axis is provided by the inequivalence of the three bridging anions; the organic groups on two of them are methyl and phenyl whereas the third has two octyl groups. (The observed structure in the adsorption band probably arises from complicated Fano effects[64] among the electronic levels and vibronic states, and does not give direct information on the lifting of the degeneracy.)

If the dipolar fields were absent the distortions would split the $^4A_{2g}$ ground state into a pair of Kramers doublets. Also, if the quantization axis for splitting the $\pm\frac{1}{2}$ levels from the $\pm\frac{3}{2}$ levels is parallel to the chain axis, the spin levels remain in doublets with dipolar fields present. Using crystal-field theory, which may not be strictly applicable due to the overlap of the chromium and oxygen orbitals, the splitting between the doublets can be calculated. Checking the g-value shift shows that the theory[39] gives reasonable results.

$$g=2(1-4\lambda/\Delta) \ . \tag{3.1}$$

Substituting the free-ion spin-orbit coupling parameter $\lambda=91$ cm^{-1} and $\Delta=15\,000$ cm^{-1} gives $g=1.95$ which does not overestimate the observed g shift too badly, $g=1.974$.[63] The anisotropy parameter is given by[39]

$$D=4\lambda^2\delta/\Delta^2 \ , \tag{3.2}$$

where δ is the orbital splitting among the $^4T_{2g}$ levels. A value for D of a few times 10^{-2} K is typical for chromium and indeed has been observed in a dimeric phosphinate which was examined in our laboratory as a crystalline model compound.[65,66] The predicted contributions to the anisotropy are thus $D/k\sim-0.1$ K from dipolar fields and $|D|/k\sim0.1$ K from the crystal field. As we shall show, these values are of the same order of magnitude as the anisotropy obtained by comparing experimental data to the numerical calculation, $|D|/k\gtrsim0.03$ from the susceptibility difference in and out of the sheet in the temperature range 1–10 K, and $|D|/k\lesssim0.03$ from the susceptibility rise below 0.5 K.

The fact that the $^4T_{2g}$ level is split into three nongenerate levels must produce an E anisotropy parameter. Although there is some evidence in the magnetic data that E is present, it does not result in a dominant effect. The reasons for the suppression of E will be discussed below.

IV. EXPERIMENTAL METHODS

The magnetic properties of PCrP-C were investigated with a variety of experimental techniques. Using a Faraday balance, an ac mutual inductance bridge and a superconducting quantum interference detector (SQUID) magnetometer, the susceptibility was measured from 20 mK to room temperature. Data for the other standard thermodynamic quantity, specific heat, were also extended into the mK range.

A. ac mutual inductance bridge

An ac mutual inductance bridge operating at 25 Hz was used to measure the differential magnetic susceptibility from 1.0 to 100 K in static fields from 0 to 50 kG. The bridge design is similar to that originally introduced by Hartshorn,[67] but several improvements have been incorporated.

The electronics are shown in Fig. 9. The real and imaginary parts of the sample susceptibility can be measured simultaneously. The sample is moved back and forth between two secondary coils and the difference voltage is recorded in order to cancel background signals, even if they are slowly drifting.

The glass tail of the cryostat (Fig. 10) fits inside the mutual inductance coils. The temperature inside the tail can be adjusted from 1.0 to over 100 K. Helium gas at one atmosphere maintains thermal contact with the sample. With the setup shown it is possible to keep the sample temperature constant within 0.1 K as it moves up and down. Below 4.2 K the inner tail and 1-K pot are filled with liquid helium and pumped. Using a manostat the sample temperature can be held constant to within 0.01 K.

An important criterion in the design of this apparatus is the combined use of a mutual inductance bridge and a superconducting magnet. This introduces several problems. Extreme care must be used to suppress microphonic noise. Also, the diamagnetic superconducting wire produces a large background signal which is very dependent upon the magnet's temperature and past field history. After changing fields, the background may drift for hours. To eliminate this signal it was necessary to move the sample back and forth between the secondary coils and take the difference signal. The background is also very noisy. This noise, which is probably due to flux jump, grows exponentially with either increasing primary field or temperature. It was reduced to an acceptable level by cooling the magnet to 2 K. Even then, the magnet noise was the major limitation on

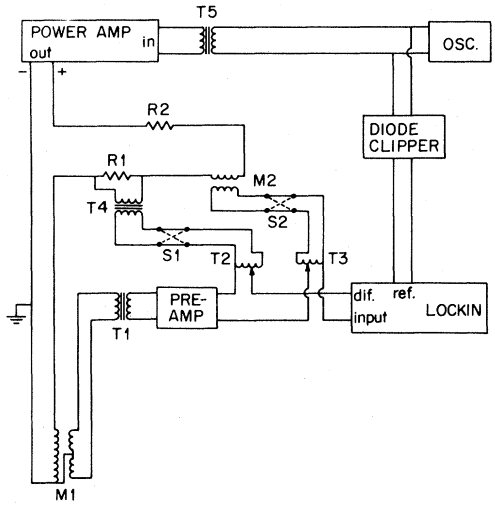

FIG. 9. Circuit diagram of modified Hartshorn bridge used for differential susceptibility measurements. The sample is moved between the secondaries of $M1$. $M2$ is a reference mutual inductance. $T2$ and $T3$ are ratio transformers used to null the imaginary and real parts, respectively, of the susceptibility signal. $T1$ is a PARC 190 low-noise transformer. $T4$ and $T5$ are UTC transformers LS-30 and LS-150, respectively. $R_1 = 0.5\ \Omega$, $R_2 = 5\ \Omega$.

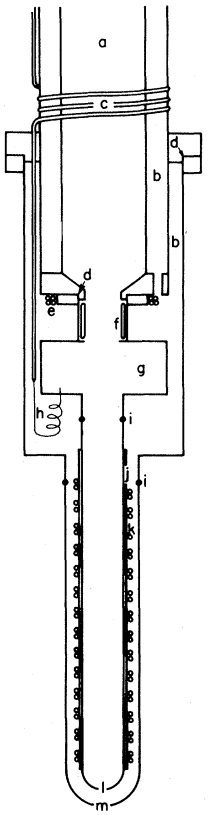

FIG. 10. Temperature controlled insert: a—pumping line; b—vacuum jacket; c—^{4}He condenser; d—lead seal; e—auxiliary heater; f—glass insert; g—1-K pot; h—capillary fill line; i—glass-to-metal seals; j— coil foil; k—heater; 1 and m—double-wall glass tail.

the system's sensitivity. The resulting sensitivity is of the order 10^{-8} (dimensionless susceptibility) and is the same (within 10%) for the real and imaginary channels.

B. Faraday balance

A Faraday balance with a computer data acquisition system was used to measure the low-field, $H \leq 10$ kG, susceptibility from 4 to 300 K. Kulick and Scott have described the setup elsewhere.[62] The electrobalance has 0.1-μg sensitivity leading to a resolution of 0.1% for samples whose susceptibility is greater than a few times 10^{-7} cm.^{3}

C. SQUID measurements

Low-temperature measurements, 20 to 700 mK, were taken with a SQUID magnetometer[68] in severa fields ranging from 3 to 469 G. It was operated in a dc mode in which at each field the SQUID responds to changes in magnetization as the temperature is swept. The sample filling factor was calculated by approximating a cylindrical sample with a coil having the same outer dimensions and using mutual inductance tables.[69]

D. Specific heat

Specific heat in zero field was measured from 80 mK to 2.8 K using the quasiadiabatic heat pulse method.[70] To shorten the internal equilibrium time, gold was evaporated on both sides of the sample sheets and the bundle of sheets was wrapped in thin copper foil.

V. EXPERIMENTAL RESULTS AND DISCUSSION (REF. 71)

A. Magnetic susceptibility; $T \gtrsim 6$ K

In Fig. 7, magnetic susceptibility data from the Faraday balance and ac inductance bridge are shown. The higher-resolution Faraday balance data were fitted from 6 to 300 K using (i) the analytic expression[48] for the classical ($S = \infty$) Heisenberg antiferromagnetic chain and (ii) numerical results[55] for the quantum $S = \frac{3}{2}$ chain. 6 K is the lowest temperature at which the effects of anisotropy, which are not included in either model, do not adversely affect the fit. Fitting parameters and statistics are presented in Table I. The quantum model yields a slightly, but statistically significantly, better fit, with the discrepancies in the classical model being most apparent at lower temperature (see Fig. 11). Moreover,

TABLE I. Comparison of statistics obtained in fitting susceptibility data $6 \leq T \leq 300$ K to predictions of classical and quantum ($S = \frac{3}{2}$) antiferromagnetic chains. Quoted standard deviations of the fitting parameters are statistical.

	Classical	$S = \frac{3}{2}$ quantum
g	2.010(1)	1.979(1)
J/k (K)	−2.775(5)	−2.486(3)
Std. dev.	1.8×10^{-4}	1.0×10^{-4}
R^2	0.999 84	0.999 95
F test	1.1×10^6	1.8×10^6

the g value obtained from ESR spectroscopy., $g_{ESR} = 1.974(1)$, is in much better aggreement with the $S = \frac{3}{2}$ g value, $g_Q = 1.98$, than with the classical value, $g_c = 2.01$. Since the Faraday balance measurements have an absolute accuracy of order 0.1%, this is a significant distinction. Hence we conclude that we are seeing the (small) quantum effects of finite spin, and that the numerical calculations of Blöte[55] provide an accurate description.

Note that the effect of quantum fluctuations is quite similar to that of static disorder, as discussed in Ref. 58, for the classical model. The susceptibility is increased, and, for fixed J, the maximum shifts to lower temperature. In view of the quality of the fit to the $S = \frac{3}{2}$ calculation, and the high degree of crystallinity observed in the x-ray diffraction and birefringence of PCrP-C we believe that, the discussion of Ref. 58 notwithstanding, disorder (i.e., randomness in the exchange) is *not* an important factor in determining the magnetic properties of this polymer.

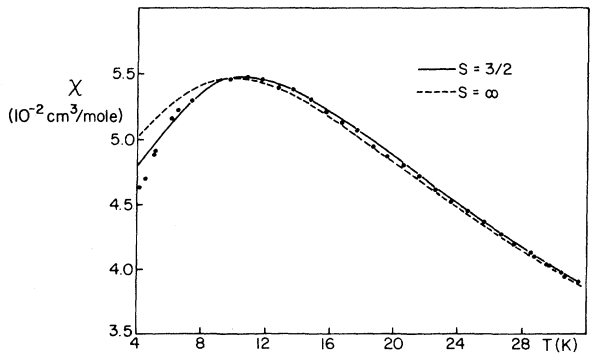

FIG. 11. Comparison of classical and quantum fits to static susceptibility of PCrP-Cr. Data were fitted for $6 \leq T \leq 300$ K. (See text and Table I.)

B. Magnetic susceptibility; $1 \lesssim T \lesssim 6$ K

Below about 6 K the effects of anisotropy begin to be evident. The initial susceptibility ac measurements ($H_{ac} < 100$ G, $H_{dc} = 0$) for the oscillating field in the plane of χ_{in} and normal to χ_{out} the sample sheets are shown in Fig. 12 (compare Fig. 2). In order to deduce whether the observed anisotropy arises from easy-axis or easy-plane behavior it is necessary to recognize that, because the chains are not completely aligned but have azimuthally random orientation within the sheet, both χ_{in} and χ_{out} involve partial averages of $\chi_\perp$ and $\chi_\parallel$. The difference $\chi_{in} - \chi_{out}$ is therefore less than $\chi_\perp - \chi_\parallel$.

If one assumes complete alignment of the molecules within the plane of the sheet, and uses the fact that the x-ray data imply completely random distribution of the chains with respect to rotation about their own axes, then the appropriate averages are

easy axis:

$$\chi_{in} = (3\chi_\perp + \chi_\parallel)/4 \ , \tag{5.1a}$$

$$\chi_{out} = (\chi_\perp + \chi_\parallel)/2 \ ; \tag{5.1b}$$

easy plane:

$$\chi_{in} = (\chi_\perp + \chi_\parallel)/2 \ , \tag{5.2a}$$

$$\chi_{out} = \chi_\parallel \ , \tag{5.2b}$$

where $\chi_\perp$ and $\chi_\parallel$ refer to perpendicular and parallel to the easy axis or easy plane, as the case may be. Note that the easy-axis case requires $\chi_\perp - \chi_\parallel$ to be twice as large to observe the same difference in susceptibility. However the initial susceptibility data are not, in themselves, sufficient to deduce the sign of the anisotropy. We shall return to this point later.

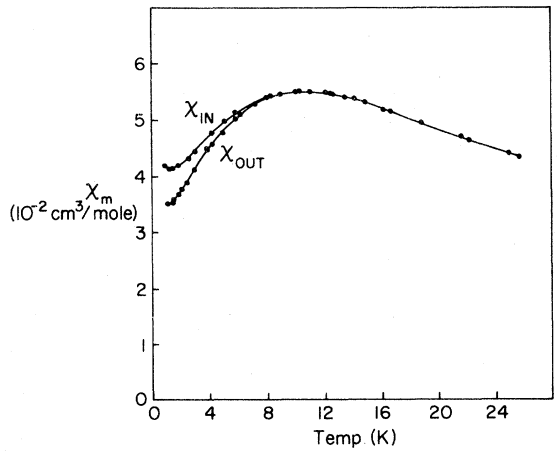

FIG. 12. Initial susceptibility of PCrP-C obtained with the ac field perpendicular (χ_{out}) and parallel (χ_{in}) to the sample sheet.

C. Field dependence of susceptibility

In Fig. 13 is shown the dependence on applied static magnetic field of the susceptibility parallel to the sample sheet (χ_{in}) and perpendicular to it (χ_{out}). Compare these data with the numerical results depicted in Fig. 3. The behavior of $\chi_{in}(H)$ and $\chi_{out}(H)$ is typical of a one-dimensional antiferromagnet above its three-dimensional Néel temperature. The susceptibility increase at high fields is indicative of a gradual crossover to spin-flopped alignment, in which the moments, which already possess short-range antiferromagnetic order, are driven perpendicular to, with slight canting towards, the field. Since the order is only short ranged the field overcomes not only anisotropy but also thermal agitation. The absence of any tendency for $\chi(H)$ to show a peak [cf. Fig. 3(a)] and the fact that the crossover field, H_{SF}, is proportional

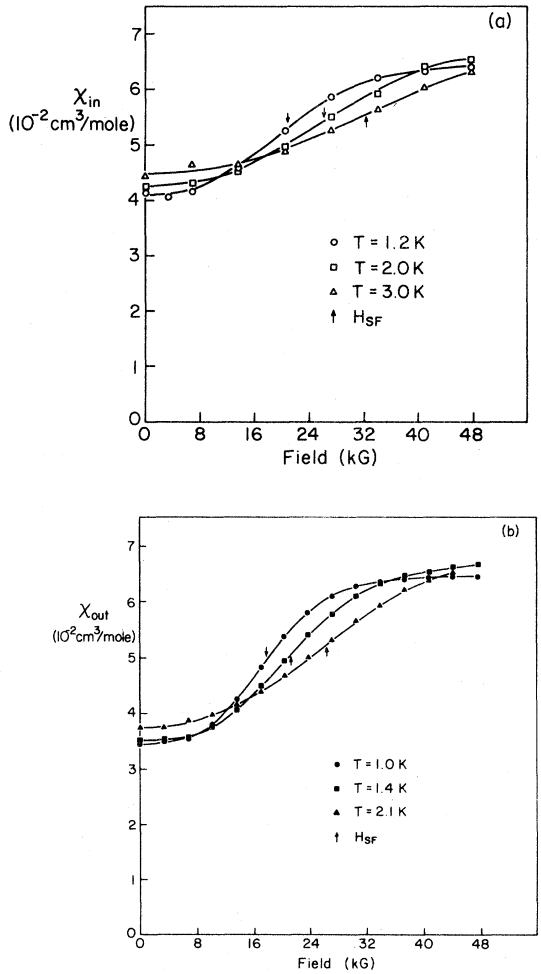

FIG. 13. Field dependence of the susceptibility at several temperatures (a) χ_{in}, (b) χ_{out}. H_{SF} is chosen as the point for 50% enhancement of the susceptibility.

to the temperature lead to the conclusion that the anisotropy is easy plane; i.e., $D < 0$. The Zeeman energy is thus inducing perpendicular alignment by competition only with thermal energy.

At very high fields ($\mu H >> kT$) the susceptibility becomes independent of orientation and of field strength: $\chi \rightarrow 6.5 \times 10^{-2}$ cm^3/mole. This is the behavior expected when the Zeeman energy competes only with the exchange energy in inducing spin alignment parallel to the applied field:

$$\lim_{\mu H >> kT} \chi = Ng^2\mu_B^2/8|J_c| \ . \tag{5.3}$$

This independent experimental result gives $J_c/k = -2.8$ K, which is in agreement with the fit to the high-temperature susceptibility (Table I).

D. Magnitude of D

Having deduced, from the field dependence of χ, that easy-plane anisotropy is acting, we now return to the temperature dependence of $\chi_{in} - \chi_{out}$ in order to evaluate its magnitude. Quantitative comparisons of theory and experiment must be made carefully for two reasons: first, as already noted, the experimental data does not yield the full difference $\chi_\perp - \chi_\parallel$; second, the theory gives only $\chi_\parallel$ for easy axis and $\chi_\perp$ for easy plane because the calculation is possible only when there is a symmetry axis. In addition, the calculations, being classical, are expected to become less accurate as the temperature decreases.

With all these caveats in mind, compare Figs. 12 and 2. In the latter, D was adjusted (J and g having been determined by the classical fit to the higher-temperature data) so that at 1 K $\chi_{in} - \chi_{out} \cong (\chi_\perp - \chi_\parallel)/2$ as required by Eq. (5.2) [using the isotropic (Heisenberg) result for $\chi_\parallel$]. The anisotropy parameter thus obtained is $D/k = -0.03$ K. We consider this estimate to be approximately 50% accurate.

Since easy-plane anisotropy prevails the field dependence of the susceptibility is insensitive to the magnitude of D and we cannot obtain an independent estimate from the data of Fig. 13.

One might argue that the peak in $\chi(H)$ for easy-axis anisotropy is smeared out by orientational averaging in PCrP-C. If this were the case then the magnitude of D would have to be twice as large to give the observed difference $\chi_{in} - \chi_{out}$. The lowest-temperature data (1 K) would then correspond roughly to curve b of Fig. 3(a). We have performed orientation averaging calculations which show that, even for a completely spherical distribution, this peak is not suppressed. Hence easy-axis anisotropy is inconsistent with the data.

E. Magnetic susceptibility $T \lesssim 1$ K

Since the value of the crossover temperature deduced from the above results is $T_A \sim (S^2JD)^{1/2} \sim 1$ K, and since knowledge of the 3D Néel temperature would be useful, we made measurements at lower temperature using a SQUID magnetometer and dilution refrigerator. Data were taken in the in-plane geometry with applied static fields ranging from 3 to 470 G. Since the SQUID responds to magnetization changes, not magnetization, a constant has been added to each field run to obtain agreement near 1 K with the ac inductance measurements. Plotting M/H vs $1/T$, Fig. 14, shows that the low-temperature, $T \lesssim 100$ mK, behavior contains a contribution attributable to isolated Curie moments, saturating for large H/T. There is also a field independent kink at about $T = 200$ mK.

The data are interpreted as the sum of the magnetization from long chains and a Curie tail, from isolated spins and very short chains, given by a Brillouin function. For chains longer than the coherence length, which at the lowest temperature is hundreds of lattice spacings, the infinite chain calculation will apply, and the susceptibility will depend mainly upon competition between the anisotropy and field and only weakly on temperature. To obtain this intrinsic behavior we have subtracted a Brillouin function from the data of Fig. 14, to give the susceptibility shown in Fig. 15. Notice that below about $T \sim 200$ mK the susceptibility begins to level off and becomes constant, within experimental error, at low tempera-

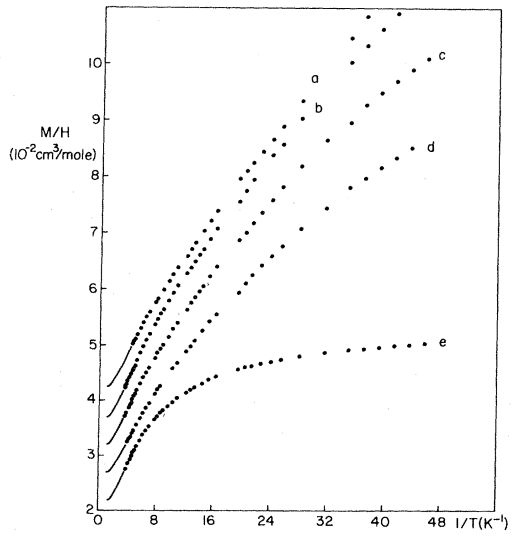

FIG. 14. Low-temperature ($T < 1$ K) magnetization data taken with a SQUID magnetometer: M/H vs $1/T$. The applied fields are (a) 3.05, (b) 14.3, (c) 33.8, (d) 65.3, and (e) 469 Oe. The solid lines between 250 mK and 1 K represent data too close to distinguish.

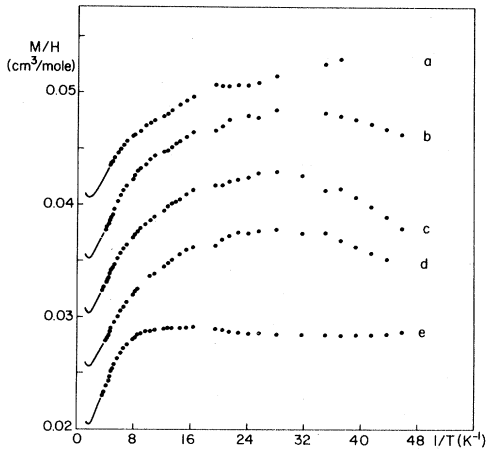

FIG. 15. Data of Fig. 14 after subtraction of a Brillouin function $B_{3/2}(H/T)$ corresponding to an isolated spin concentration of 0.06%.

ture. The Curie constant used in the subtraction varied from 0.0014 cm^3 K/mole at 3 G to 0.0012 cm^3 K/mole at 470 G, indicating a concentration of isolated spins and chains fragments of 0.06%. Thus the samples used are magnetically very clean, and the upturn in χ_{in} at low temperature is not the typical "Curie tail," but shows the effects of anisotropy. The slight variation in the Curie constant probably reflects contributions from chains which are close to the coherence length and so have a more complicated field and temperature dependence.

There is no evidence of an additional anomaly in the low-temperature susceptibility which could be attributed to three-dimensional ordering.

F. Specific heat

Further evidence favoring the description in terms of crossover from Heisenberg to XY spin symmetry is given by the specific heat. The change in entropy associated with the reduction in spin dimensionality occurs at such a low temperature that the magnetic contribution dominates that from the lattice.

In Fig. 16 experimental data are shown along with numerical results from a quantum $S=\frac{3}{2}$ Heisenberg calculation[44] using $J_Q/k=-2.5$ K and with a low-temperature linear extrapolation of those results. In order to obtain the coefficient of the linear term we have extended the numerical results smoothly to zero temperature, while requiring that the total entropy at high temperature be $S(T\rightarrow\infty)=R\ln(2S-1)$. The coefficient of the linear term thus obtained is 0.084 K^{-1} (i.e., $C/R=0.21kT/|J_Q|$). This value should be contrasted with the semiclassical prediction of Kubo,[72] $C/R=0.35kT/|J|$.

The extrapolation fits the midtemperature,

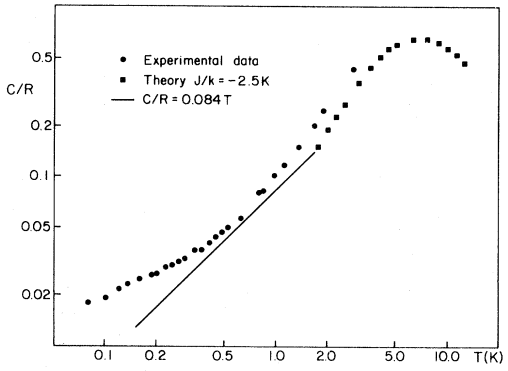

FIG. 16. Specific heat of PCrP-C. The theoretical points are taken from numerical work of Blöte (Ref. 44). The linear extrapolation is explained in the text. Note the logarithmic scales.

$T\sim0.7$ K, data very well whereas the semiclassical result does not. At higher temperature the increase above the numerical curve is consistent with a T^3 lattice contribution. At lower temperature there is clearly an additional contribution to the specific heat, over and above the linear spin-wave term.

The low-temperature data with the linear term subtracted are shown in Fig. 17, on the same tempera-

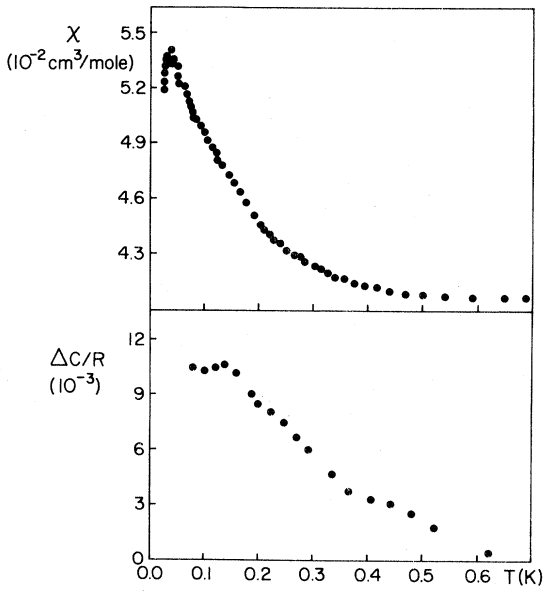

FIG. 17. (a) Field-independent part of the susceptibility of PCrP-C. The data points are identical to those of Fig. 15(b), but shown on a linear temperature scale. The downturn at low temperature is probably not significant, since the errors in the temperature scale approach 10%. (b) "Excess" specific heat in PCrP-C, obtained as the difference between the data of Fig. 16 and the linear low-temperature extrapolation.

ture scale as the intrinsic susceptibility data (taken from Fig. 15). It is clear that the excess specific heat must be associated with the entropy change involved in the crossover to an anisotropic magnetic system at low temperature. Unfortunately quantitative comparison with the results of the classical transfer-matrix calculation are not enlightening, but we do see qualitative behavior in Figs. 2(b) and 4(b) similar to that of Fig. 17.

There are (at least) three other possible origins of the excess specific-heat anomaly, two of which can be immediately discounted. First is a Schottky anomaly due to the ^{31}P (and perhaps ^{1}H) nuclei in the hyperfine field of the Cr ions. The magnitude of this hyperfine field has been determined[73] by NMR to be 4.6 kG, which yields a specific heat two orders of magnitude smaller than observed. Second, the contribution from isolated electronic moments (e.g., Cr ions) in ligand or dipolar fields would be, on the basis of the known impurity concentration (0.06%), at least an order of magnitude too small.

It is more difficult to rule out three-dimensional ordering due to the weak (dipole-dipole perhaps) interaction between spins on neighboring chains. Such ordering might be smeared by residual structural disorder and might not lead to an observable anomaly in the susceptibility. We can use the x-ray data, which indicates structural coherence parallel to the chains in excess of 20 lattice spacings, to conclude that ordering above about 1 K, where $\xi/a \cong 2|J| \times S(S+1)/kT \cong 20$, would lead to sharp features in both C and χ. Below 1 K the increase in C and χ might be due to a smeared 3D ordering, but we believe that the overall consistency of the data with the picture of Heisenberg-XY crossover weighs against this. Remember that the parameters of the symmetry crossover model were obtained from the higher ($T > 1$ K) data.

In the absence of any direct evidence of a Néel temperature down to 20 mK, we can put a lower limit on the "one-dimensionality factor" $T_{MF}/T_{3D} > 10^3$. This make PCrP-C "better" than TMMC, where $T_{MF} = 80$ K and $T_{3D} = 0.85$ K,[17] and comparable to α-CuNSal, where $T_{MF} = 3$ K and $T_{3D} < 3$ mK.[32]

G. What happened to E?

The structural evidence implies that the chromium environment was distorted sufficiently that an anisotropy parameter E should be present. Yet in our description of the data we found no evidence that E is important. We believe that this is due to the fact that there is some degree of disorder in the orientation of the E axis in the XY planes perpendicular to the molecular axis. This will arise because the octylphosphinate groups, which break the threefold symmetry around the chain axis, are randomly located. Hence, when the coherence length of the antiferromagnetic order exceeds the correlation length of this structural arrangement the anisotropy energy associated with E will tend to average to zero.

Conversely at higher temperature the anisotropy energy acting on a small cluster of spins will be the sum of the D and E contributions and the onset of anisotropy will appear more quickly. This is precisely what is observed qualitatively by comparing Fig. 2(a) with Fig. 12. Put another way: a larger anisotropy parameter is required at high temperature than at low to reproduce the observed difference between χ_{in} and χ_{out}.

VI. CONCLUSION

The experimental data on PCrP-C may be summarized as follows:

(i) The initial susceptibility is that of a Heisenberg antiferromagnetic chain at high temperature and shows increasing anisotropy below about 6 K.

(ii) The susceptibility increases with applied field in a manner consistent with easy-plane anisotropy, i.e., $\mu H_{SF} \sim kT$ and there is no peak.

(iii) The crossover from isotropic spin symmetry to XY behavior which commences at about 6 K is not complete until below 100 mK, as observed in the low-temperature susceptibility and specific heat.

These experimental data and the theoretical analysis presented in Sec. II show that, within the short-range-ordered paramagnetic state of a one-dimensional antiferromagnet, there is a rich variety of behavior which springs from the competition among exchange anisotropy, Zeeman and thermal energies. For the material which we have examined, PCrP-C, the exchange interaction $|J|/k = 2.5$ K giving a mean-field temperature of order 20 K. The anisotropy is found to be easy plane with a magnitude $|D|/k \sim 0.03$ K, which value is consistent with the expectations of both single-site anisotropy and dipolar interactions. The characteristic temperature, T_A, signaling the crossover from Heisenberg to XY symmetry is thus computed to be of order 1 K, but we note that the crossover region is rather wide, extending from approximately 100 mK to 6 K. (The calculation shows that similar behavior may be expected in the change from Heisenberg to Ising behavior for easy-axis anisotropy.)

We have found no evidence for the onset of a three-dimensional ordering at low temperature, although we cannot completely rule out the possibility that the transition is smeared by residual disorder. The primary argument against such a picture lies with the good, albeit only semiqualitative, agreement between the theory of anisotropy and experiment. Therefore one concludes that PCrP-C is an example of a system in which anisotropy is more important than three-dimensional coupling. This anisotropy, enhanced by collective exchange effects, leads to a

crossover in spin symmetry above the Néel temperature. The origin of the anisotropy lies in part with the distortion of the chromium environment from octahedral symmetry, and in part with the dipolar interaction along the chain. Similar effects have been seen, but not so thoroughly explored, in TMMC[14,17,74] and in $CsMnCl_3 \cdot 2H_2O$.[75,76]

Given that the spin symmetry is continuous ($n=2$ for XY and 3 for Heisenberg), the effect, at low temperature, of increasing magnetic field, is to induce a continuous change to a spin-flopped-like alignment. The characteristic field associated with this change is predicted and found to be proportional to temperature. It would be amusing to find an easy-axis one-dimensional antiferromagnet in which, below $kT_A \sim \sqrt{|JD|}$, the spin-flop field is given by $\mu H_{SF} \sim \sqrt{|JD|}$.

The overall agreement between the experimental data and the numerical results, although convincing, is by no means perfect. We attribute this discrepancy to the fact that the calculation deals with a classical model so that quantum fluctuations are not taken into account. The classical results are known to be in extreme error for the low-temperature specific heat, and we have shown also that discrepancy in the susceptibility between classical and quantum models amounts to some 10% near T_{MF} and increases at lower temperature.

ACKNOWLEDGMENTS

This work was supported by the Cornell Materials Science Center, NSF-MRL Grant No. DMR-76-81083. The authors wish to express their gratitude to Professor R. H. Silsbee and Dr. P. D. Krasicky for numerous enlightening discussions, and for making available their data prior to publication. Dr. D. A. Kurtze gave invaluable guidance in numerical methods for the transfer-matrix calculation. Dr. H. W. J. Blöte kindly provided results of his numerical calculations prior to publication.

[1]L. J. de Jongh and A. R. Miedema, Adv. Phys. 23, 1 (1974).
[2]D. W. Hone and P. M. Richards, Ann. Rev. Mat. Sci. 4, 337 (1974).
[3]M. Steiner, J. Villain, and C. G. Windsor, Adv. Phys. 25, 87 (1976).
[4]J. C. Bonner, J. Appl. Phys. 49, 1299 (1978).
[5]For example, K. W. H. Stevens, in *Magnetism*, edited by G. T. Rado and H. Suhl (Academic, New York, 1963), Vol. 1, p. 1.
[6]W. Heisenberg, Z. Phys. 49, 619 (1928).
[7]E. Ising, Z. Phys. 31, 253 (1925).
[8]E. H. Lieb, T. Schultz, and D. C. Mattis, Ann. Phys. (N.Y.) 16, 407 (1961).
[9]N. D. Mermin and H. Wagner, Phys. Rev. Lett. 17, 1133 (1966).
[10]L. D. Landau and E. M. Lifshitz, *Statistical Physics*, 2nd ed. (Addision-Wesley, Reading, Mass., 1969), p. 478.
[11]D. J. Scalapino, Y. Imry, and P. Pincus, Phys. Rev. B 11, 2042 (1975).
[12]Y. Imry, P. Pincus, and D. Scalapino, Phys. Rev. B 12, 1978 (1975).
[13]See for example, J. Kanamori, in *Magnetism*, edited by G. T. Rado and H. Suhl (Academic, New York, 1963), Vol. 1, p. 127.
[14]R. Dingle, M. E. Lines, and S. L. Holt, Phys. Rev. 187, 643 (1969).
[15]R. J. Birgeneau, R. Dingle, M. T. Hutchings, G. Shirane, and S. L. Holt, Phys. Rev. Lett. 26, 718 (1971).
[16]M. T. Hutchings, G. Shirane, R. J. Birgeneau, and S. L. Holt, Phys. Rev. B 5, 1999 (1972).
[17]L. R. Walker, R. E. Dietz, K. Andres, and S. Darack, Solid State Commun. 11, 593 (1972).
[18]C. Dupas and J.-P. Renard, Phys. Lett. A 43, 119 (1973).
[19]P. M. Richards, Phys. Rev. B 10, 805 (1974).
[20]W. J. M. de Jonge, C. H. W. Swuste, K. Kopinga, and K. Takeda, Phys. Rev. B 12, 5858 (1975).
[21]J.-P. Boucher, M. A. Bakheit, M. Nechtschein, M. Villa, G. Bonera, and F. Borsa, Phys. Rev. B 13, 4098 (1976).
[22]T. T. P. Cheung, Z. G. Soos, R. E. Dietz, and F. R. Merritt, Phys. Rev. B 17, 1266 (1978).
[23]N. Achiwa, J. Phys. Soc. Jpn. 27, 561 (1969).
[24]M. Melamud, H. Pinto, J. Makowsky, and H. Shaked, Phys. Status Solidi (b) 63, 699 (1974).
[25]H. Rinneberg and H. Hartman, J. Chem. Phys. 52, 5814 (1970).
[26]C. F. Putnik and S. L. Holt, Inorg. Chem. 16, 1010 (1977).
[27]W. Breitling, W. Lehmann, T. P. Srinivasan, R. Weber, and U. Durr, Solid State Commun. 24, 267 (1977).
[28]E. C. Lingafelter, G. L. Simmons, B. Morosin, C. Sheringer, and C. Freiburg, Acta Crystallogr. 14, 1222 (1961).
[29]R. R. Bartkowski, J. Hennessy, B. Morosin, and P. M. Richards, Solid State Commun. 11, 405 (1972).
[30]R. R. Bartkowski and B. Morosin, Phys. Rev. B 6, 4209 (1972).
[31]R. C. Knauer and R. R. Bartkowski, Phys. Rev. B 7, 450 (1972).
[32]L. J. Azevedo, W. G. Clark, D. Hubin, and E. O. McLean, Phys. Lett. A 58, 255 (1976).
[33]L. J. Azevedo, A. Narath, P. M. Richards, and Z. G. Soos, Phys. Rev. Lett. 43, 875 (1979).
[34]M. Steiner and H. Dachs, Solid State Commun. 9, 1603 (1971).
[35]M. Steiner and B. Dorner, Solid State Commun. 12, 537 (1973).
[36]J. V. Lebesque, J. Snel, and J. J. Smit, Solid State Commun. 13, 371 (1973).
[37]M. Steiner, B. Dorner, and J. Villain, J. Phys. C 8, 165 (1975).
[38]J. K. Kjems and M. Steiner, Phys. Rev. Lett. 41, 1137 (1978).
[39]B. N. Figgis, *Introduction to Ligand Fields* (Interscience, New York, 1966).

[40]For example: L. N. Bulaevskii, Sov. Phys. JETP 16, 685 (1963); 17, 684 (1963) [Zh. Eksp. Theor. Fiz. 43, 968 (1962); 44, 1008 (1963)].
[41]J. C. Bonner and M. E. Fisher, Phys. Rev. 135, A640 (1964).
[42]T. de Neef and W. J. M. de Jonge, Phys. Rev. B 11, 4406 (1975).
[43]T. de Neef, Phys. Rev. B 13, 4141 (1976).
[44]H. W. J. Blöte, Physica (Utrecht) 78, 302 (1974); Physica (Utrecht) B 79, 427 (1975); 93, 93 (1978).
[45]J. des Cloiseaux and J. J. Pearson, Phys. Rev. 128, 2131 (1962).
[46]R. B. Griffiths, Phys. Rev. 133, A768 (1964); 135, A659 (1964).
[47]T. Nakamura, J. Phys. Soc. Jpn. 7, 264 (1952).
[48]M. E. Fisher, Am. J. Phys. 32, 343 (1964).
[49]G. S. Joyce, Phys. Rev. Lett. 19, 581 (1967).
[50]H. E. Stanley, Phys. Rev. 179, 570 (1969).
[51]J. M. Loveluck, S. W. Lovesey, and S. Aubry, J. Phys. C 8, 3841 (1975).
[52]M. Blume, P. Heller, and N. A. Lurie, Phys. Rev. B 11, 4483 (1975).
[53]W. Pesch and W. Selke, Z. Phys. B 23, 271 (1976); W. Selke and W. Pesch, *ibid.* 24, 203 (1976).
[54]C. Y. Weng, thesis (Carnegie-Mellon University, 1968) (unpublished).
[55]H. W. J. Blöte (private communication).
[56]B. P. Block, Inorg. Macromol. Rev. 1, 115 (1970).
[57]J. C. Scott, Ph.D. thesis (University of Pennsylvania, 1975) (unpublished).
[58]J. C. Scott, A. F. Garito, A. J. Heeger, P. Nannelli, and H. D. Gillman, Phys. Rev. B 12, 356 (1975).
[59]T. S. Wei, J. C. Scott, A. F. Garito, A. J. Heeger, H. D. Gillman, and P. Nannelli, Phys. Rev. B 12, 5297 (1975).
[60]J. C. Scott, T. S. Wei, A. F. Garito, A. J. Heeger, H. D. Gillman, and P. Nannelli, in *Magnetism and Magnetic Materials-1975 (Philadelphia),* edited by J. J. Becker, G. H. Lander and J. J. Rhyne, AIP Conf. Proc. No. 29 (AIP, New York, 1975), p. 506.
[61]P. Nannelli, H. D. Gillman, and B. P. Block, J. Polym. Sci. Polym. Chem. Ed. 13, 2849 (1975).
[62]J. D. Kulick and J. C. Scott, J. Vac. Sci. Technol. 15, 800 (1978).
[63]P. D. Krasicky and R. H. Silsbee (private communication).
[64]M. D. Sturge, H. J. Guggenheim, and M. H. L. Pryce, Phys. Rev. 32, 2459 (1970).
[65]P. D. Krasicky, J. C. Scott, R. H. Silsbee, and A. L. Ritter, J. Phys. Chem. Solids 39, 991 (1978).
[66]R. Cini, P. Orioli, H. D. Gillman, and P. Nannelli, Cryst. Struct. Commun. 8, 621 (1979).
[67]L. Hartshorn, J. Sci. Instrum. 2, 145 (1925).
[68]C. M. Bastuscheck, Ph.D. thesis (Cornell University, 1980) (unpublished).
[69]F. W. Grover, *Inductance Calculations: Working Formulas and Tables* (Dover, New York, 1962).
[70]A. K. Raychaudhuri, Ph.D. thesis (Cornell University, 1980) (unpublished).
[71]Preliminary reports of this work have been given by R. E. Stahlbush and J. C. Scott, J. Appl. Phys. 50, 1664 (1979); Solid State Commun. 33, 707 (1980).
[72]R. Kubo, Phys. Rev. 87, 568 (1952).
[73]L. S. Smith, P. R. Newman, A. J. Heeger, A. F. Garito, H. D. Gillman, and P. Nannelli, J. Chem. Phys. 66, 5428 (1977).
[74]D. Hone and A. Pires, Phys. Rev. B 15, 323 (1977).
[75]T. Smith and S. A. Friedberg, Phys. Rev. 176, 660 (1968).
[76]K. Nagata, Y. Tazuke, and K. Tsushima, J. Phys. Soc. Jpn. 32, 1486 (1972).